Egyptian Knowledge Bank
https://ijmti.journals.ekb.eg/

International Journal of Materials Technology and Innovation
Volume 4, Issue 1 (2024), pages 32-41

Online ISSN 2682-4299

A brief review of silver phosphate nanocomposites as photocatalysts

Sabrin M. Abdo [1,2,*], Soliman I. El-Hout [1], Mohamed Nageeb Rashed [2] Thanaa I. El-Dosoqy [2] and Said M. El-Sheikh [1,]**

[1] Nanostructured Materials and Nanotechnology Department, Advanced Materials Institute, Central Metallurgical R&D Institute (CMRDI) P.O. Box 87 Helwan, Cairo 11421, Egypt
[2] Chemistry Department, Faculty of Science, Aswan University, Aswan, 81528, Egypt

*Corresponding author: E-mail: houria_algazira@yahoo.com (Sabrin M. Abdo)
**Corresponding author: E-mail: selsheikh2001@gmail.com (Said M. El-Sheikh)

Received ……20 May 2024
Accepted …… 9 June 2024
Published …....13 June 2024

Abstract

The photocatalytic destruction of organic dyes and contaminants using semiconductor photocatalysts has been widely investigated for water purification. However, the requirement for UV light for photocatalyst activation hinders its practical applicability due to its low percentage in solar light; consequently, enhancing its activity is critical. To prevent this issue, bandgap adjustment can be processed by the introduction of metal or non-metal dopants or the production of composites of diverse materials. Silver phosphate is an outstanding visible-light-driven semiconductor photocatalyst, demonstrating exceptional photoactivity for water splitting and degradation of pollutants in aqueous solution. Though the photocorrosion phenomena of Ag_3PO_4 limit its application, Ag_3PO_4-based photocatalysis was able to overcome this phenomenon and expand the scope of application for treating polluted water. This study summarized the techniques made in this subject to remove barriers to practical implementation and improve photocatalytic performance. The various strategies for synthesizing Ag_3PO_4 and different nanocomposites were then discussed.

Keywords: Silver phosphate; photocatalysis; wastewater treatment; nanocomposite; photodegradation.

1. Introduction

Water is vital to both ecosystems and human societies. Human actions have a massive, pervasive impact on the environment. However, many people do not have access to safe and clean water to drink, and many die as an effect of water-borne bacterial diseases. Water covers more than two-thirds of the earth's surface; however, it is predominantly salty and hazardous for human consumption. Freshwater accounts for 2.7% of the world's potential water resources, although only 1% of that freshwater (found in lakes, rivers, and groundwater) is accessible. The fundamental cause of environmental contamination is the disruption of the ecological balance between humans and nature. Even trace levels of hazardous compounds and dyes dumped into waterways can influence aquatic life and the food chain. Organic pollutants such as dyes, antibiotic compounds, and heavy metals, which are widely employed in the textile, rubber, paper, cosmetic, pharmaceutical, paint, leather, food, plastic, and other sectors, have contributed significantly to the deterioration of the environment, particularly water pollution [1]. The treatment of wastewater is emerging as an urgent issue worldwide as a result of a lack of safe drinking water, population growth, and a rise in water-polluting sectors such as petroleum refineries, textile factories, and medical centers. Waste pollutants are classified into three types: microbial contaminants, mineral contaminants, and organic pollutants [2]. Efficient approaches for eliminating organic components from water have

IJMTI vol. 4, issue 1 (2024) 32-41 https:// doi: 10.21608/IJMTI.2024.291301.1104

piqued interest. Synthesis of nanomaterials with established shapes is critical for optimizing their properties and applications. The use of nanomaterials is being addressed in a variety of fields, one of which is directly related to ecology via photocatalysis.

Silver phosphate (Ag_3PO_4), also known as silver orthophosphate, is a water-insoluble yellow chemical compound produced from the interaction of soluble silver salt with orthophosphate [3]. Silver phosphate precipitation is similarly utilized in silver staining of biological materials as a phosphate enlarging agent and as a light-sensitive agent in early photography, besides its antibacterial effects. Ag_3PO_4 is a photocatalyst driven by visible light. It displays a band gap energy equal to 2.43 eV [4]. Pristine Ag_3PO_4 photocatalyst may absorb solar light energy with wavelengths less than 530 nm and has a VB close to +2.9 V compared to a standard hydrogen electrode (SHE, pH = 0), indicating an exceptional oxidizing capability. Furthermore, silver phosphate has an extraordinary quantum yield (90%) for photo-chemically splitting water under visible light and generating activated oxygen by the same technique [5]. Due to these advantages of Ag_3PO_4 photocatalysts, as well as the drawbacks such as self-corrosion, lots of synthesis methods have been proposed to fabricate Ag_3PO_4-based nanocomposites [6-14]. Those developed nanocomposites display superior activity compared to pristine silver phosphate for environmental applications.

2. Synthesis of silver phosphate

A simple precipitation procedure employing silver nitrate and Na_2HPO_4 as precursors resulted in spherical Ag_3PO_4. Under visible light, the as-prepared materials displayed substantial efficiency in the photocatalytic destruction of Rhodamine B. Photocatalytic activity increased initially but eventually decreased as recycle times increased. A probable mechanism for the improvement and subsequent falls of Ag_3PO_4 photocatalytic activity is hypothesized based on systematic particle characterization utilizing X-ray diffraction (XRD), X-Ray Photoelectron Spectroscopy (XPS), Scanning Electron Microscopy (SEM), Transmission Electron Microscopy (TEM), and UV/Vis absorption spectroscopy. Spherical Ag_3PO_4 particles were effectively recycled four times, while Ag nanoparticles coated with silver phosphate served as electron capture centers, lowering the recombination rate of electron-hole pairs. Increased recycling times reduce photocatalytic efficiency because of the shielding impact of Ag nanoparticle coatings on the Ag_3PO_4 surface [15].

A simple chemical deposition approach on a polycarbonate (PC) template resulted in highly consistent Ag_3PO_4 nanorods of varying sizes. Nanorods produced using a PC membrane with different hole widths had diameters of 2.0 µm, 275 nm, or 85 nm. The features, structures, chemical compositions, and photocatalytic properties of prepared Ag_3PO_4 nanorods were carefully examined. Under visible light, Ag_3PO_4 nanorods displayed remarkable photocatalytic efficiency towards methylene blue, Congo Red, and rhodamine B. Only nanorods with a diameter of 275 nm had the highest photocatalytic performance due to the combined effects of their shape and size [16].

The photocatalytic efficacy of Ag_3PO_4 was reported under visible light treatment using methylene blue (MB) as a model pollutant. Water is used as a solvent in the ion-exchange and hydrothermal techniques for producing Ag_3PO_4. XRD, Field Emission Scanning Electron Microscope (FE-SEM), Fourier-transform infrared spectroscopy (FTIR), Ultraviolet-Visible Diffuse Reflectance Spectroscopy (UV-Vis DRS), Thermogravimetric and differential thermal analysis (TG-DTA), and Impedance spectroscopy describe the as-prepared Ag_3PO_4. Finally, Ag_3PO_4 products were employed as photocatalysts for methylene blue photodegradation under visible light. The dye-dependent degradation is studied using different photocatalyst doses of Ag_3PO_4. Compared to hydrothermally synthesized Ag_3PO_4, the photodegradation outcomes demonstrate that all doses of Ag_3PO_4 assembled by ion-exchange synthesis technique show complete photodegradation with a short time of irradiation. It also has minimal electric resistance that encourages a greater number of photo-generated electron-hole pairs, which has a significant impact on the photodecomposition of MB [17].

A simple ion-exchange approach was used to generate Ag_3PO_4 photocatalysts in two and one steps. XRD, SEM, and UV-vis (DRS) were applied to investigate the photocatalysts. The catalytic efficacy of the photocatalysts was determined by the photocatalytic decomposition of methyl orange and methylene blue under sunlight irradiation. The photocatalyst synthesized through the two-step ion-exchange approach had a MO degradation rate of 89.18% in 60 minutes, four times that of the photocatalyst prepared in a single step. In 40 minutes, the photodegradation rate of MB was 97%, while MO

IJMTI vol. 4, issue 1 (2024) 32-41 https:// doi: 10.21608/IJMTI.2024.291301.1104

degradation rate was 73% after six after six cycling runs [18].

Precipitation, ion exchange, soft-chemical, and hydrothermal methods have all been used to create variously shaped Ag_3PO_4 photocatalysts. To establish a link between surface attributes and photoactivity, the samples were examined for morphological characteristics, structure of the crystals, particular surface area, optical characteristics, and photoactivity for degradation of phenol under visible light illumination. When branching and rhombic dodecahedral Ag_3PO_4 particles were present, the degradation rate was similar to that in the case of P25 under UV light. According to the results of the photodegradation intermediates analysis, benzoquinone was the major by-product of phenol degradation. Scavenger-supported photocatalytic experiments indicated that under visible radiation, typically O_2- was involved in phenol decomposition. While the XPS surface composition study revealed that greater silver content promotes photoactivity, whereas a higher Ag^0/Ag^+ ratio inhibits photoactivity [19].

Ag_3PO_4 nanoparticles were synthesized and used as photocatalysts in the photocatalytic degradation of numerous dyes (Rhodamine B, Methylene blue, Methyl orange, and Orange G) and drugs (SMZ). Many analytical instruments, such as Powder X-ray Diffraction (PXRD), FTIR, UV-Vis DRS, Dynamic Light Scattering Particle Size Distribution Analysis (DLS), FE-SEM, and high-resolution transition electron microscope (HR-TEM), were employed to investigate the photocatalyst. The chemical interaction of dye molecules with photocatalyst surfaces has been investigated to comprehend the photodecomposition reaction pathway. All organic dyes and pharmaceuticals exhibited pseudo-first-order reactions, and it was discovered that the photocatalyst degraded Rhodamine B dye and SMZ drug rapidly. The highest recorded photodegradation rate for the SMZ drug was 0.0744 min-1, while for RhB, it was 0.0532 min-1. The minimal degradation rate for OG dye was measured to be 0.0036 min-1, which is 15 times lower than that of RhB dye. According to the findings of the comparative dye degradation study, an organic pollutant's photodegradation effectiveness is dependent on the photocatalyst surface charge. The impact of photo-generated reactive species was similarly investigated using various kinds of scavengers that aided in explaining photochemical processes and photocatalyst mechanisms. The optimal photocatalyst under light irradiation was also used to analyze genuine samples of textile effluent [20].

The widespread use of Ag_3PO_4 is unsurprising, given its superior photostability compared to other silver-based compounds. The current study focuses on a simple approach for precipitating silver phosphate (Fig. 1). The influence of four distinct phosphate suppliers (H_3PO_4, NaH_2PO_4, Na_2HPO_4, and $Na_3PO_4.12$ H_2O) as well as two starting concentrations (0.1 and 0.2 M) were studied. The basic nature of the various phosphate suppliers affects the purity degree of Ag_3PO_4, resulting in multiple end products. H_3PO_4 did not result in the synthesis of Ag_3PO_4. However, NaH_2PO_4 produced Ag_3PO_4 and a minor amount of pyrophosphate. The acquired samples' morphological and structural features were investigated using XRD, DRS, SEM, FTIR, and XPS spectroscopy. The degradation of methyl orange under visible light was utilized to evaluate the materials' photocatalytic activity and reaction kinetics. Reusability experiments, Photoluminescence (PL) studies, and characterization following deterioration were all used to investigate their stability. The deposited Ag nanoparticles also had an impact on the stability and recycling of Ag_3PO_4. Although it restricted the development of holes and decreased the photodegradation of MO, they did not affect the photocatalyst's performance [21].

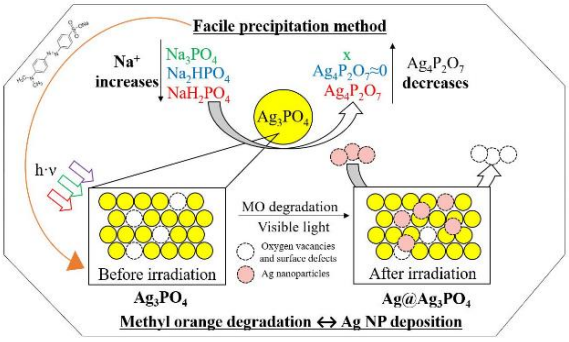

Fig. 1 Synthesis approach and degradation mechanism [21].

3. Synthesis of silver phosphate nanocomposites

The in-situ growth approach using organic solvent established graphene-modified nanosized Ag_3PO_4 photocatalyst. When compared to Ag_3PO_4 nanoparticles and large-sized Ag_3PO_4 particles-graphene composites, the as-prepared Ag_3PO_4 nanoparticles-graphene composite demonstrated

IJMTI vol. 4, issue 1 (2024) 32-41 https:// doi: 10.21608/IJMTI.2024.291301.1104

boosted photocatalytic efficiency and stability towards the degradation of MB in aqueous solution under irradiation of visible light. This improved photocatalytic efficacy and photostability result from the favorable synergistic impact of Ag_3PO_4 nanoparticles and graphene sheets, which include increasing the active adsorption sites, inhibiting electron-hole recombination, and lowering Ag nanoparticle production [22].

An in-situ deposition approach was utilized to create a Z-Scheme $Ag_3PO_4/Ag/WO_{3-x}$ photocatalyst. $WO_{2.72}$, with a hierarchical sea urchin-like assembly, was initially combined with an excess of Ag^+ ions. The $WO_{2.72}$'s low reducibility was used to convert Ag^+ to Ag in situ, and then Ag nanoparticles were dropped on the surface of $WO_{2.72}$. Following that, a sufficient quantity of PO_4^{3-} ions was directly injected to react with the residual Ag+ ions, resulting in the in-situ deposition of Ag3PO4 nanoparticles on the Ag/WO_{3-x} surface and formation of Z-Scheme $Ag_3PO_4/Ag/WO_{3-x}$ photocatalyst. The outcomes show that for the Z-Scheme $Ag_3PO_4/Ag/WO_{3-x}$ photocatalyst, Ag nanoparticles act as carrier-transfer centers, significantly extending the lifetime of the photo-generated electrons of Ag_3PO_4 and the photo-generated holes of WO_{3-x}, and thus improving the photocatalytic efficiency [23].

Using a solvothermal-liquid phase deposition technique, a new composite photocatalyst ($Ag_3PO_4/ZnFe_2O_4$) with improved photocatalytic performance was synthesized for the first time. Kinetic investigations on the composite's photodegradation of 2,4-dichlorophenol (2,4-DCP) revealed that $Ag_3PO_4/ZnFe_2O_4$ (mass ratio was 9:1, respectively) exhibited a measurable rate constant that equal 9.95 times comparable to $ZnFe_2O_4$ also equal 3.15 times that of Ag_3PO_4. Furthermore, during a 70-min irradiation, the 2,4-DCP mineralization rate reflected by the total organic carbon removal rate (% TOC) reached around 48 %. The photocatalytic pathway of the composite is similarly studied, and the improved photocatalytic performance is due to the effective separation of charge carriers as well as the modified size of the new composite [24].

An ultrasonication/chemisorption approach was used to create Ag_3PO_4@g-C_3N_4core@shell nanocomposites. The catalytic capability of Ag_3PO_4@g-C_3N_4 nanocomposites was estimated by studying the decomposing of MB. After 30 minutes of irradiation, the Ag_3PO_4@g-C_3N_4 sample demonstrated the highest photocatalytic efficacy, decomposing 97% MB. In the cyclic runs, outstanding stability was also observed. The prepared composite has exceptional photocatalytic performance and photostability, with an optimum g-C_3N_4 content of 7.0 wt.%. Photocurrent and EIS measurements indicated that the effective electron-hole separation resulted from a robust interaction in the close contact interface. A photocatalytic pathway of organics decomposition over Ag_3PO_4@g-C_3N_4 photocatalysts was suggested, dependent on the outcomes of experiments [25].

To produce the EB-Ag_3PO_4 photocatalyst, a nanophase of Ag_3PO_4 was disseminated on exfoliated bentonite (EB). All prepared samples were investigated using XRD, TEM, FTIR, UV-vis, DRS, and the Brunauer-Emmett-Teller (BET) technique. The composites were created by spreading very fine Ag_3PO_4 nanoparticles on exfoliated thin bentonite layers to enhance photocatalytic efficiency by increasing surface area with Ag_3PO_4. On a per mole basis of Ag_3PO_4, an optimal EB-Ag_3PO_4 composite degraded rhodamine B significantly faster than pristine Ag_3PO_4 under visible light. Furthermore, corresponding to the kinetics of degradation data, compositing with exfoliated bentonite appeared to boost the degradation efficiency of Ag_3PO_4. Under visible light illumination, the RhB decomposition over EB-Ag_3PO_4 composite was around 95% within 21 minutes, which is significantly better than that of Ag_3PO_4 (82%). The increased activity was due mainly to the electrostatic interaction between the positive and negative charges on Ag_3PO_4 and exfoliated bentonite, respectively, and the effective motion of charge carriers in the composite [26].

An in-situ synthesis technique was used to deposit Ag_3PO_4 nano-sized particles on the Ag_2S two-dimensional sheet surface. Surface-functioned Ag_2S sheets could modify the microstructure, composition, and efficiency of the generated Ag_3PO_4/Ag_2S composites. The composite performed better when the molar ratio between Ag_2S and Ag_3PO_4 was 0.31, resulting in a 2-fold increase in degradation rate compared to pure Ag_3PO_4. A Z-scheme system was established to efficiently separate charge carriers, with Ag nanoparticles as a combination center of CB-e^- of Ag_3PO_4 and VB-h^+ of Ag_2S. Besides the matching band structure of both Ag_2S and Ag_3PO_4, the presence of Ag_2S made dispersed Ag_3PO_4 nanoparticles effective in light capture. The beneficial interface effect created by Ag_2S sheets, as well as Ag_3PO_4 nanoparticles, additionally assists in boosting photocatalytic performance [27].

IJMTI vol. 4, issue 1 (2024) 32-41 https:// doi: 10.21608/IJMTI.2024.291301.1104

A simple precipitation method was employed to establish a unique modified nanocomposite from Ag_3PO_4 (AP), Ag_2S, and reduced graphene oxide (G) (Fig. 2). The physicochemical characteristics and optical features of the materials were investigated using XRD, FT-IR, Raman spectra, HR-TEM, XPS, UV-Vis, and PL spectroscopy. The prepared nanocomposites had boosted visible-light responsiveness, lower band gap energy, and a fast electron-hole separation rate. The photocatalytic effectiveness of modified Ag_3PO_4 nanocomposites was investigated for reduction of Cr(VI) in aqueous solution under visible light irradiation. During 45 minutes of illumination as well as a dose of 0.05 g/L, the optimized composite with 20 wt% Ag_2S achieved a boosting efficiency for reduction of 98.7% for Cr(VI) and a rate constant of 0.0734 min^{-1}, nearly 49 times greater than that of pure AP. The XPS measurement of the wasted catalyst confirmed the unique Cr(III) peaks. Furthermore, the nanocomposite demonstrated significant recycling four times with minimal activity loss. Finally, the mechanism of photoreduction for the nanocomposite was proposed [28].

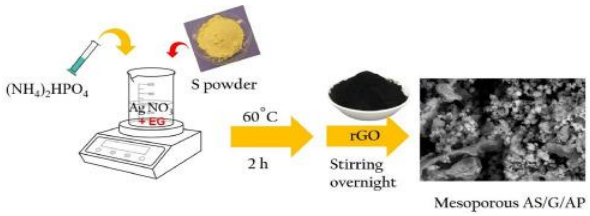

Fig. 2 Preparation approach of $Ag_2S/G/Ag_3PO_4$ nanocomposites [28].

Both techniques of co-precipitation hydrothermal and oxidative polymerization were used to successfully synthesize Ag_3PO_4 photocatalysts modified with $BiPO_4$ and polypyrrole (PPy). SEM, Energy-dispersive X-ray spectroscopy (EDS), TEM, BET, XRD, FT-IR, XPS, UV-vis DRS, Electrochemical Impedance Spectroscopy (EIS), and photocurrent techniques were used to investigate their morphologies, structures, and optical and electronic features. Malachite green was selected as a model organic pollutant to evaluate Ag_3PO_4-$BiPO_4$-PPy heterostructures' photocatalytic efficacy and stabilities under visible light illumination. The outcomes demonstrated that $BiPO_4$ and PPy considerably affected photocatalytic efficacy and significantly boosted Ag_3PO_4 photostability in continual and long-term applications. Ag_3PO_4-$BiPO_4$-PPy heterostructures had a degradation conversion equal to 1.58 times that of pristine Ag_3PO_4, and the photo-corrosion of Ag_3PO_4 was successfully prevented. After five repeated cycles, photocatalytic efficiency was around 87% in Ag_3PO_4-$BiPO_4$-PPy heterostructures, whereas pristine Ag_3PO_4 can only conserve about 33% of the degradation efficiency. This paper also examined the possible pathway of increased stability and catalytic efficiency of Ag_3PO_4-$BiPO_4$-PPy heterostructures [29].

A simple precipitation approach was employed to prepare sulfate-doped Ag_3PO_4 photocatalysts successfully. XRD and XPS analysis indicated that SO_4^{2-} ions were integrated into the Ag_3PO_4 lattice by substituting PO_4^{3-}. After SO_4^{2-} -doping, the crystal morphology and optical absorption performance of Ag_3PO_4 stay unaffected. However, an SO_4^{2-}doped Ag_3PO_4 catalyst with an SO_4^{2-} ratio of 0.50 % degraded RhB and MB completely in 4 and 5 minutes, respectively, when exposed to visible light. Its degradation rate was higher 5 times than that of pure Ag_3PO_4. The outstanding photocatalytic efficiency is due to the incorporation of SO_4^{2-} into the Ag_3PO_4 lattice, which enhanced the separation efficiency of charge carriers and inhibited their recombination. Furthermore, density functional theory studies show that SO_4^{2-} can successfully adjust the electronic structures of Ag_3PO_4, leading to significant photocatalytic performance when exposed to visible light [30].

A reaction between Ag_3PO_4 dodecahedrons and Na2S solutions through an in-situ anion-exchange approach created sequences of Ag_2S/Ag_3PO_4 nanocomposites with definite core/shell geometries. The acquired nanocomposites were analyzed using X-ray diffraction, BET, AFS, SEM, TEM, EDX, XPS, DRS, and PL spectroscopy. Using visible and near-IR light irradiation, Ag_2S/Ag_3PO_4 nanocomposites demonstrated good photocatalytic efficacy for MO degradation. The best nanocomposite, Ag_2S-5%/Ag_3PO_4, displayed the most excellent visible-light-driven performance, degrading virtually all MO during 120 minutes. After 240 minutes of exposure to near-IR light, the Ag_2S-50%/Ag_3PO_4 composite exhibited the highest photocatalytic efficiency. Recycling tests indicated that the Ag_2S/Ag_3PO_4 nanocomposites outperformed in cycle performance and photostability. The Ag_2S content and core/shell configuration strongly influenced the photocatalytic performance. The improved photocatalytic efficiency of Ag_2S/Ag_3PO_4 composites could be generally attributed to the effective separation of electron-hole pairs at the

IJMTI vol. 4, issue 1 (2024) 32-41 https:// doi: 10.21608/IJMTI.2024.291301.1104

interface of the Ag_2S shell and the Ag_3PO_4 core. During the photodegradation process, the produced Ag nanoparticles at the surfaces of Ag_3PO_4 and Ag_2S operated as charge transmission bridges as well as electron capture centers, respectively, establishing stable $Ag_2S/Ag/Ag_3PO_4$ Z-scheme system and $Ag/Ag_2S/Ag_3PO_4$ ternary system. The probable photocatalytic pathways for MO degradation under both visible and near-IR light illumination over Ag_2S/Ag_3PO_4 composites were hypothesized based on the experiment's outcomes [31].

Spherical Ag_3PO_4 as well graphene oxide (GO) wrapped Ag_3PO_4 (Ag_3PO_4@GO) nanocomposites with varying GO concentrations were effectively prepared using simple co-precipitation and ultrasonic procedures. The materials' morphology, structure, and surface bonds were investigated using SEM, TEM, X-ray diffraction, FT-IR Spectroscopy, and XPS spectroscopy. The photocatalytic efficacy of these materials towards rhodamine B (RhB) decomposition was also investigated under visible light. The Ag_3PO_4 hybrid with 0.01 g GO (Ag_3PO_4@10GO) had the highest Ag vacancies content, enhancing the best photocatalytic activity [32].

Silver phosphate (Ag_3PO_4) loading over titanium dioxide (TiO_2: P25)-coated silicon (SiO_2) felt resulted in heterostructured photocatalyst ($Ag_3PO_4/TiO_2/SiO_2$). Owing to its relatively small bandgap energy of 2.5 eV, this heterostructure improved its ability to absorb light. As a result, it demonstrated improved photocatalytic performance in degrading methylene blue under sunlight irradiation (30% and 10% vs. pure P25 and P25-coated SiO_2 felt, respectively). The optimal degradation efficacy for methylene blue was 99%. The estimated quantum yield of $Ag_3PO_4/TiO_2/SiO_2$ (3.26×10^{-3} molecules/photon) was seriously superior compared to that of other systems (~3260 times other mentioned heterostructures, rGO/TiO_2, Ni-doped/TiO_2, and $Cds/CoFe_2O_4$) with excellent recycling. As a result, $Ag_3PO_4/TiO_2/SiO_2$ nanocomposite is recommended for efficiently remedying organic contaminants in wastewater systems [33].

The deposition of silver phosphate on diatomite resulted in the development of tiny Ag_3PO_4 particles on diatomite surfaces, forming diatomite-Ag_3PO_4 (DT/AgP) composites with varying DT/AgP ratios. UV-vis. DRS study data revealed that DT/AgP composites can absorb visible wavelengths, but TiO_2 catalysts can only work in UV light. Using BET analysis, the composite samples have a higher specific surface area than pure AgP. The photocatalytic process displayed a pseudo-first-order rate reaction; also, the nanocomposite with DT/AgP ratio 1:0.8 has superior catalytic activity for the decomposition of RhB and MO. Deposition of silver phosphate clusters on diatomite might be assumed to produce an effective photocatalyst triggered by sunlight irradiation [34].

Silver phosphates, as well as their composites, have piqued researchers' attention as photocatalysts with possible antimicrobial properties. The current study sought to understand the mechanism of bactericidal activity in cells of opportunistic infections. The Ag_3PO_4/P25 (AGP/P25) and Ag_3PO_4/HA (HA/AGP) powders were created using a co-precipitation process. Then, their antibacterial activities against Enterococcus faecalis, Staphylococcus epidermidis, and Staphylococcus were tested in the dark and after exposure to visible light (VIS). Transmission electron microscopy and scanning transmission electron microscopy with energy-dispersive X-ray spectroscopy were used to examine the bacterial cells' morphological alterations. It has been demonstrated that Ag_3PO_4 composites are very effective photocatalysts capable of eliminating 100% of bacterial populations during the 60-minute photocatalytic inactivation. Their principal effect is the formation of $OH^{\bullet}$ and h^+, which causes oxidative stress in cells (Fig. 3) [35].

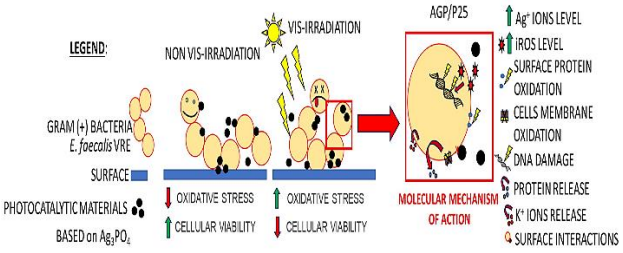

Fig. 3 The mechanism of the tested photocatalytic materials based on Ag_3PO_4 against Gram-positive bacteria [35].

This study emphasizes the photodecomposition of organic pollutants, specifically methylene blue dye, as well as the creation of hydrogen as a green energy source utilizing a photocatalyst composed of silver phosphate Ag_3PO_4 and barium oxide/silver phosphate BaO@Ag_3PO_4. This composite was effectively manufactured utilizing a chemical co-precipitation method. The obtained samples' physicochemical properties were studied utilizing SEM, EDX, XRD, FT-IR, UV-Vis/DRS, and PL spectrophotometry. According to XRD, the typical crystalline sizes of AP

IJMTI vol. 4, issue 1 (2024) 32-41 https:// doi: 10.21608/IJMTI.2024.291301.1104

and APB are 39.1 and 46 nm, respectively. UV and PL tests demonstrated that the compound is visible light photoactive, with a decrease in recombination rate in the presence of BaO and Ag_3PO_4 (Fig. 4). After 120 minutes of illumination, the as-prepared photocatalyst sample demonstrated a 94% decomposition efficacy of MB (20 ppm, 50 mL) and a hydrogen production yield of 7538 µmol/(h•g), exceeding that of AP sample's 88% efficiency. The remarkable photodecomposition effectiveness was related to the electronic enhancement action of BaO particles. When exposed to visible light, the APB composite showed improved photocatalytic efficiency in the complete decomposition of organic dye (MB) [36].

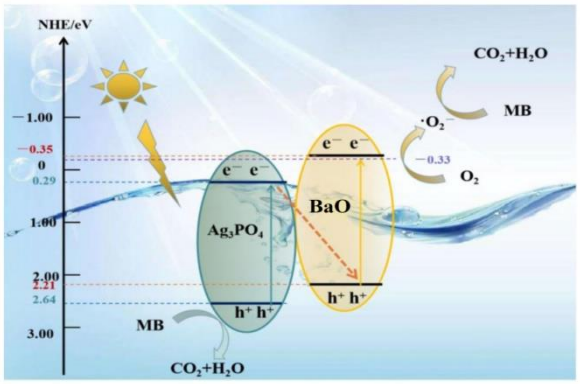

Fig. 4 Diagram of the photocatalytic proposed mechanism of BaO@Ag_3PO_4 nanocomposite under visible light illumination [36].

Silver phosphate (Ag_3PO_4) was used to coat titania-silica (TiO_2-SiO_2) microspheres, resulting in a solar light active photocatalyst. Titania-silica microspheres were created by spray drying TiO_2-SiO_2 colloidal solutions, and Ag_3PO_4 was added through wet impregnation. XRD and SEM investigation displays that silver phosphate nanoparticles deposited on the surface of the titania-silica microspheres (Fig. 5) and UV-vis. DRS reveals that Ag_3PO_4/TiO_2-SiO_2 composites can excited by visible light. BET measurements demonstrate that composite samples have a greater specific surface area than bare Ag_3PO_4. Dye degradation studies were conducted under solar light irradiation to assess photocatalytic activity. In a dye photodegradation experiment under solar light illumination, the produced photocatalysts adhere to a pseudo-first-order rate law. The results reveal that the composite catalysts with an Ag_3PO_4/TiO_2-SiO_2 ratio of 1:1.6 wt% demonstrate superior photocatalytic efficacy for both RhB and MO degradation [37].

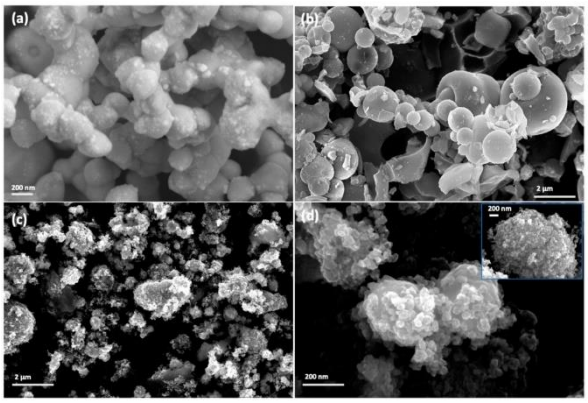

Fig. 5 SEM images of (a) Ag_3PO_4, (b) TS82, (c) TS82-AgP16, and (d) higher resolution image of TS82-AgP16 [37].

The photocatalytic method based on Ag_3PO_4 has tremendous promise for eliminating antimicrobial contaminants, but the poor separation rate of charge carriers limits its applicability. In the current study, it was discovered that combining nitrogen-doped carbon (NDC) with carbon defects and Ag_3PO_4 can considerably improve Ag_3PO_4's photocatalytic activity. After 5 minutes of exposure to visible light, the composite photocatalyst Ag_3PO_4@NDC achieved 100% photocatalytic degradation of oxytetracycline. Furthermore, SEM, TEM, XRD, Raman, and Electron paramagnetic resonance spectroscopy (EPR) were used to characterize the structures of NDC, Ag_3PO_4, and Ag_3PO_4@NDC. A potential strategy for increasing the photocatalytic reaction of the Ag_3PO_4@NDC composite catalyst was postulated (Fig. 6). The current study gives a superior visible light photocatalytic material, which can be a useful reference for fabricating and preparing a new superior visible light photocatalytic [38].

Chemical precipitation was used to create a tube-like g-C_3N_4/ Ag_3PO_4 nanocomposite. Ag_3PO_4 nanoparticle was deposited onto the tube-like g-C_3N_4 (TCN) surface, resulting in intimate contact (Fig. 7). The photodegradation of RhB determined the catalytic effectiveness of as-prepared photocatalyst under visible light illumination. The tube-like g-C_3N_4/Ag_3PO_4-5% heterojunction demonstrated excellent photocatalytic activity. In an ideal approach, the RhB photodecomposition rate is 90% after 40 minutes of visible-light irradiation. After five successive runs, the recycling experiment revealed that the activity of the tube-like g-C_3N_4/Ag/Ag_3PO_4-5% heterojunction remained unchanged. A potential Z-type mechanism is

IJMTI vol. 4, issue 1 (2024) 32-41 https:// doi: 10.21608/IJMTI.2024.291301.1104

postulated to clarify the high photoactivity and photostability of the heterojunction [39].

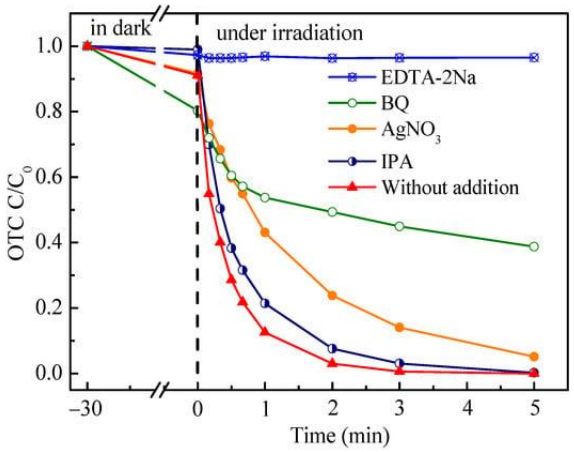

Fig. 6 Photodegradation curve of oxytetracycline by Ag_3PO_4@5 mL NDC composite photocatalyst using different scavengers [38].

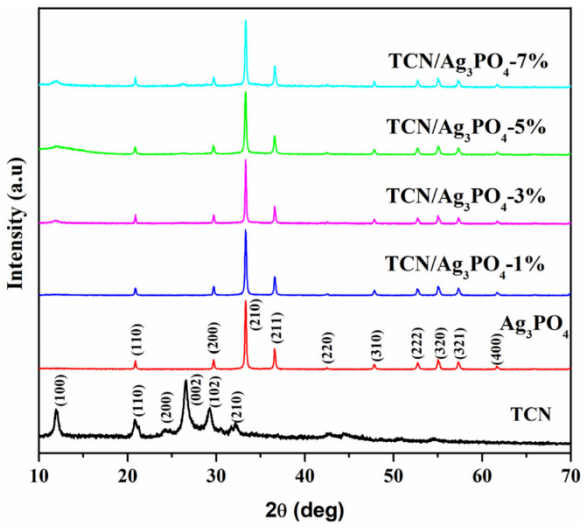

Fig. 7 XRD spectra of TCN, Ag_3PO_4, and prepared heterojunctions [39].

Ag_3PO_4-TiO_2-graphene oxide nanocomposites were synthesized using ion exchange and photocatalytic reduction techniques. The composites' characteristics and photocatalytic efficiency were explored, as well as the mechanism of photodegradation. The high content of TiO_2 nanoparticles in the nanocomposites improved light absorption but increased impedance and reduced charge transport. On the other hand, excess TiO_2 nanoparticles dispersed over Ag_3PO_4 and graphene oxide surfaces decreased the surface area and consequently depressed light absorption. A suitable TiO_2 content improved catalytic activity. A molar ratio of 0.6 Ag_3PO_4 to TiO_2 resulted in the best photodecomposition activity, evolution of hydrogen, and anti-bacterial activation. Trapping tests revealed that $O_2^{\bullet}$ and h^+ are mainly active species in the photodecomposition process (Fig. 8) [40].

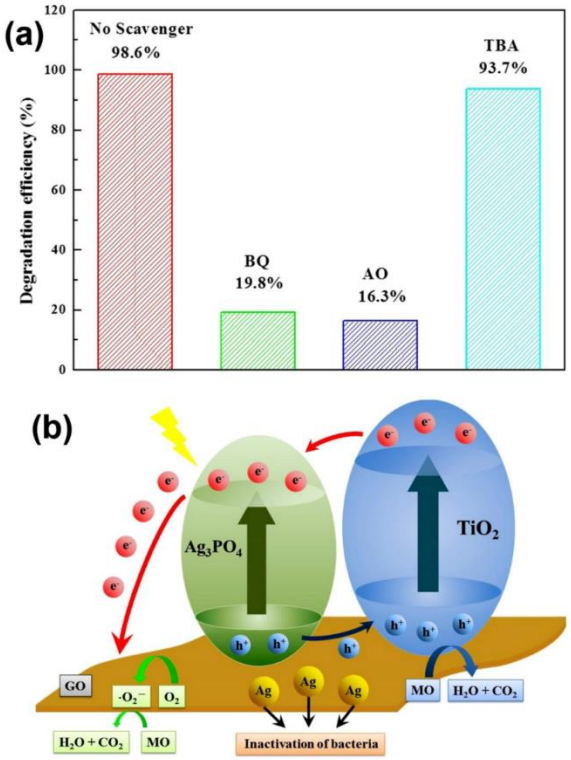

Fig. 8 (a) Trapping tests using APTGO-0.6; (b) Proposed photocatalytic mechanism of the ternary composites [40].

4. Conclusions

The study explores the use of semiconductor photocatalysts for water purification, focusing on the degradation of organic dyes and contaminants. However, the need for UV light for activation is a challenge due to its low solar light content. To overcome this, bandgap adjustment can be achieved through metal or non-metal dopants or composite materials. Silver phosphate is a notable visible-light-driven photocatalyst, demonstrating exceptional photoactivity for water splitting and pollutant degradation. The study discusses various strategies for synthesizing Ag_3PO_4 and nanocomposites.

IJMTI vol. 4, issue 1 (2024) 32-41 https:// doi: 10.21608/IJMTI.2024.291301.1104

References

[1] Joshi, Naveen Chandra, and Prateek Gururani. 2022. 'Advances of graphene oxide based nanocomposite materials in the treatment of wastewater containing heavy metal ions and dyes', Current Research in Green and Sustainable Chemistry, 5: 100306.

[2] Etacheri, V.; Di Valentin, C.; Schneider, J.; Bahnemann, D.; Pillai, S.C. Visible-light activation of TiO2 photocatalysts: Advances in theory and experiments. J. Photochem. Photobiol. C Photochem. Rev. 2015, 25, 1–29.

[3] Maatallah, N., M. Taouza and S. SOUILEM (2021). Synthèse et caractérisation physique et chimique de l'oxyde de phosphore, UNIVERSITE AHMED DRAIA-ADRAR.

[4] Yi, Z., J. Ye, N. Kikugawa, T. Kako, S. Ouyang, H. Stuart-Williams, H. Yang, J. Cao, W. Luo and Z. Li (2010). "An orthophosphate semiconductor with photooxidation properties under visible-light irradiation." Nature materials 9(7): 559-564.

[5] Yi, Z., J. Ye, N. Kikugawa, T. Kako, S. Ouyang, H. Stuart-Williams, H. Yang, J. Cao, W. Luo, Z. Li, Y. Liu and R. L. Withers (2010). "An orthophosphate semiconductor with photooxidation properties under visible-light irradiation." Nature Materials 9(7): 559-564.

[6] Abdo, Sabrin M., Soliman I. El-Hout, Mohamed Nageeb Rashed, Thanaa I. El-Dosoqy, and Said M. El-Sheikh (2024). "Boosting visible-light photodegradation of methyl orange and ibuprofen over rGO-supported Ag3PO4 nanocomposite." Inorganic Chemistry Communications 161: 112035.

[7] VG Deonikar, PV Rathod, AM Pornea, H Kim (2020) "Superior decontamination of toxic organic pollutants under solar light by reduced graphene oxide incorporated tetrapods-like Ag3PO4/MnFe2O4 hierarchical composites." Journal of Environmental Management 256 (15): 109930.

[8] A Kaitheri, SK Padmanabhan, S Pal, M Stoppa, A Licciulli (2023) "Silver phosphate–bacterial cellulose nanocomposites as visible light photocatalyst for wastewater purification." Carbohydrate Polymer Technologies and Applications 6: 100365.

[9] S.S. Patil, M.S. Tamboli, V.G. Deonikar, G.G. Umarji, J.D. Ambekar, M.V. Kulkarni, S.S. Kolekar, B.B. Kale, D.R. Patil (2015) "Magnetically separable Ag3PO4/NiFe2O4 composites with enhanced photocatalytic activity." Dalton Transactions 44: 20426-20434.

[10] X. Ke, J. Zhang, K. Dai, J. Lv, C. Liang (2019) "Novel visible-light-driven direct Z-scheme Zn3V2O8/Ag3PO4 heterojunctions for enhanced photocatalytic performance." Journal of Alloys and Compounds 799: 113-123.

[11] X. Miao, X. Yue, X. Shen, Z. Ji, H. Zhou, G. Z hu, J. Wang, L. Kong, M. Liu, C. Song (2018) "Nitrogen-doped carbon dot-modified Ag3PO4/GO photocatalyst with excellent visible-light-driven photocatalytic performance and mechanism insight." Catalysis Science & Technology 8 : 632-641.

[12] G Li, J Guo, Y Hu, Y Wang, J Wang, S Zhang and Q Zhong (2021) "Facile synthesis of the Z-scheme graphite-like carbon nitride/silver/silver phosphate nanocomposite for photocatalytic oxidative removal of nitric oxides under visible light." Journal of Colloid and Interface Science 588: 110-121.

[13] J. Ma, D. Huang, W. Zhang, J. Zou, Y. Kong, J. Zhu, S.J.C. Komarneni (2016) "Nanocomposite of exfoliated bentonite/g-C3N4/Ag3PO4 for enhanced visible-light photocatalytic decomposition of Rhodamine B." Chemosphere 162: 269-276.

[14] X. Ma, H. Li, Y. Wang, H. Li, B. Liu, S. Yin, T . Sato (2014) "Substantial change in phenomenon of "self-corrosion" on Ag3PO4/TiO2 compound photocatalyst." Applied Catalysis B: Environmental 158: 314-320.

[15] Wang, W., B. Cheng, J. Yu, G. Liu and W. Fan (2012). "Visible-light photocatalytic activity and deactivation mechanism of Ag3PO4 spherical particles." Chemistry–An Asian Journal 7(8): 1902-1908.

[16] Li, X.-Z., K.-L. Wu, C. Dong, S.-H. Xia, Y. Ye and X.-W. Wei (2014). "Size-controlled synthesis of Ag3PO4 nanorods and their high-performance photocatalysis for dye degradation under visible-light irradiation." Materials Letters 130: 97-100.

[17] Dhanabal, R., A. Chithambararaj, S. Velmathi and A. C. Bose (2015). "Visible light driven degradation of methylene blue dye using Ag3PO4." Journal of Environmental Chemical Engineering 3(3): 1872-1881.

[18] Li, J., X. Ji, X. Li, X. Hu, Y. Sun, J. Ma and G. Qiao (2016). "Preparation and photocatalytic degradation performance of Ag3PO4 with a two-step approach." Applied Surface Science 372: 30-35.

[19] Zwara, J., E. Grabowska, T. Klimczuk, W. Lisowski and A. Zaleska-Medynska (2018). "Shape-dependent enhanced photocatalytic effect under visible light of Ag3PO4 particles." Journal of Photochemistry and Photobiology A: Chemistry 367: 240-252.

[20] Kadiya, K., S. B. Vuggili, U. K. Gaur and M. Sharma (2021). "Comparative photocatalytic dye and drug degradation study using efficient visible light–induced silver phosphate

IJMTI vol. 4, issue 1 (2024) 32-41 https:// doi: 10.21608/IJMTI.2024.291301.1104

nanoparticles." Environmental Science and Pollution Research 28(34): 46390-46403.

[21] Tóth, Z.-R.; Debreczeni, D.; Gyulavári, T.; Székely, I.; Todea, M.; Kovács, G.; Focșan, M.; Magyari, K.; Baia, L.; Pap, Z.; et al. Rapid Synthesis Method of Ag3PO4 as Reusable Photocatalytically Active Semiconductor. *Nanomaterials* 2023, *13*, 89.

[22] Xiang, Q., D. Lang, T. Shen and F. Liu (2015). "Graphene-modified nanosized Ag3PO4 photocatalysts for enhanced visible-light photocatalytic activity and stability." Applied Catalysis B: Environmental 162: 196-203.

[23] Bu, Y., Z. Chen and C. Sun (2015). "Highly efficient Z-Scheme Ag3PO4/Ag/WO3−x photocatalyst for its enhanced photocatalytic performance." Applied Catalysis B: Environmental 179: 363-371.

[24] Chen, X., Y. Dai and W. Huang (2015). "Novel Ag3PO4/ZnFe2O4 composite photocatalyst with enhanced visible light photocatalytic activity." Materials Letters 145: 125-128.

[25] Liu, L., Y. Qi, J. Lu, S. Lin, W. An, Y. Liang and W. Cui (2016). "A stable Ag3PO4@g-C3N4 hybrid core@shell composite with enhanced visible light photocatalytic degradation." Applied Catalysis B: Environmental 183: 133-141.

[26] Ma, J., Q. Liu, L. Zhu, J. Zou, K. Wang, M. Yang and S. Komarneni (2016). "Visible light photocatalytic activity enhancement of Ag3PO4 dispersed on exfoliated bentonite for degradation of rhodamine B." Applied Catalysis B: Environmental 182: 26-32.

[27] Ma, P., H. Yu, Y. Yu, W. Wang, H. Wang, J. Zhang and Z. Fu (2016). "Assembly of Ag 3 PO 4 nanoparticles on two-dimensional Ag2S sheets as visible-light-driven photocatalysts." Physical Chemistry Chemical Physics 18(5): 3638-3643.

[28] Abdo, Sabrin M., Soliman I. El-Hout, Mohamed Nageeb Rashed, Thanaa I. El-Dosoqy, and Said M. El-Sheikh. 2024. 'Modified silver phosphate nanocomposite as an effective visible-light-driven photocatalyst in the reduction of aqueous Cr(VI)', Materials Research Bulletin, 169: 112511.

[29] Cai, L., H. Jiang and L. Wang (2017). "Enhanced photostability and photocatalytic activity of Ag3PO4 via modification with BiPO4 and polypyrrole." Applied Surface Science 420: 43-52.

[30] Cao, W., Z. Gui, L. Chen, X. Zhu and Z. Qi (2017). "Facile synthesis of sulfate-doped Ag3PO4 with enhanced visible light photocatalystic activity." Applied Catalysis B: Environmental 200: 681-689.

[31] Tian, Jun, Tingjiang Yan, Zheng Qiao, Linlin Wang, Wenjuan Li, Jinmao You, and Baibiao Huang. 2017. 'Anion-exchange synthesis of Ag2S/Ag3PO4 core/shell composites with enhanced visible and NIR light photocatalytic performance and the photocatalytic mechanisms', Applied Catalysis B: Environmental, 209: 566-78.

[32] Liu, R., H. Li, L. Duan, H. Shen, Q. Zhang and X. Zhao (2018). "The synergistic effect of graphene oxide and silver vacancy in Ag3PO4-based photocatalysts for rhodamine B degradation under visible light." Applied Surface Science 462: 263-269.

[33] Raza, N., W. Raza, H. Gul, M. Azam, J. Lee, K. Vikrant and K.-H. Kim (2020). "Solar-light-active silver phosphate/titanium dioxide/silica heterostructures for photocatalytic removal of organic dye." Journal of Cleaner Production 254: 120031.

[34] Padmanabhan, S. K., S. Pal and A. Licciulli (2020). "Diatomite/silver phosphate composite for efficient degradation of organic dyes under solar radiation." Bulletin of Materials Science 43(1): 295.

[35] Paluch, E.; Seniuk, A.; Plesh, G.; Widelski, J.; Szymański, D.; Wiglusz, R.J.; Motola, M.; Dworniczek, E. Mechanism of Action and Efficiency of Ag3PO4-Based Photocatalysts for the Control of Hazardous Gram-Positive Pathogens. Int. J. Mol. Sci. 2023, 24, 13553.

[36] Selim, H.; Sheha, E.R.; Elshypany, R.; Raynaud, P.; El-Maghrabi, H.H.; Nada, A.A. Superior Photocatalytic Activity of BaO@Ag3PO4 Nanocomposite for Dual Function Degradation of Methylene Blue and Hydrogen Production under Visible Light Irradiation. Catalysts 2023, 13, 363.

[37] Pal, S.; Padmanabhan, S.K.; Kaitheri, A.; Epifani, M.; Licciulli, A. Efficient Solar Light Photocatalyst Made of Ag3PO4 Coated TiO2-SiO2 Microspheres. *Nanomaterials* 2023, *13*, 588.

[38] Tong, S.; Liu, Z.; Lin, Y.; Yang, C. Highly Enhanced Photocatalytic Performances of Composites Consisting of Silver Phosphate and N-Doped Carbon Nanomesh for Oxytetracycline Degradation. *Int. J. Environ. Res. Public Health* 2022, *19*, 14865.

[39] Yan, X.; Wang, Y.; Kang, B.; Li, Z.; Niu, Y. Preparation and Characterization of Tube-like g-C3N4/Ag3PO4 Heterojunction with Enhanced Visible-Light Photocatalytic Activity. *Crystals* 2021, *11*, 1373.

[40] Sheu, F.-J.; Cho, C.-P.; Liao, Y.-T.; Yu, C.-T. Ag3PO4-TiO2-Graphene Oxide Ternary Composites with Efficient Photodegradation, Hydrogen Evolution, and Antibacterial Properties. *Catalysts* 2018, *8*, 57.